Table of Content

A

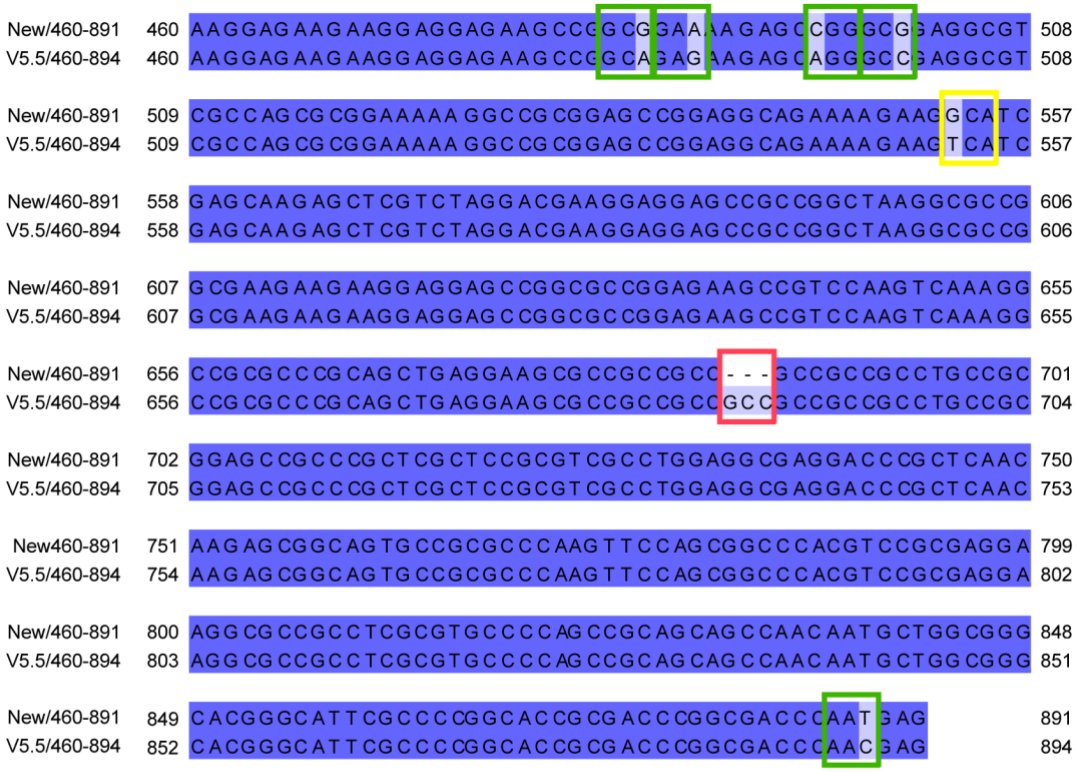

B

```
MCDNWQATIDTLQGASPVFDKPKLSQKLLEKPPFRFLHDVVTAVQQATGFAPGLYQGDELDGKAIQEKDA
KVAYLKKIIEVVSMVLGEQCPARPNKIVAGLEPENTNIFLQMLGRACQKGNGAKAVQKVLGGGGAEPAPA
KEEAPPPEKKPEKKEKKEEKPAEKSRAEASPARKKAAEPEAEKKASSKSSSRTKEEPPAKAPAKKKEEPA
PEKPSKSKAAPAAEEAPPPPPPAAEPPARSASPGGEDPLNKSGSAAPKFQRPTSARKAPPRVPQPQQPTM
LAGTGIRPGTATRRPNEPKPTDSKVTKPVAVFTDNAKDNSDDEVEVVHEQTPVLSGGANMTGEQGVLVKD
ILAAEKGLKKAGVDATADNADTSDQGSTGIILKRLGGKAAGAGAAAAGPRAHDPSSVRELVQKLCHSSTP
LAKSMDYLQEDIENMRKEYKFWLTEKRMYQDELARELRLQGEAANVDAQLADLDGQIKQARDRIIGMKGQ
ILRNDETLGKLLAMATAGR
```

Appendix Figure S1. Sequence discrepancy of IFT54 between the genome and our sequencing data.

By comparing our sequencing data of genomic DNA and cDNA of *IFT54* with that of *Chlamydomonas* V5.5 in Phytozome, we found some discrepancies. A total of seven changes in the coding sequence were found, which include five silent changes, one missense change and one deletion. (A) Partial sequence alignment showing where and what changes occur. (B) Deduced amino acids of IFT54 from our data. Highlighed amino acids indicate where the changes occur. Serine at position 185 is changed to alanine; One proline at position 230 is missing in a cluster of seven prolines 227-233, resulting in six prolines (227-232). Because of missing one of the amino acids, the total number of amino acids of IFT54 is 509 aa in stead of 510 aa as reported in Phytozome.

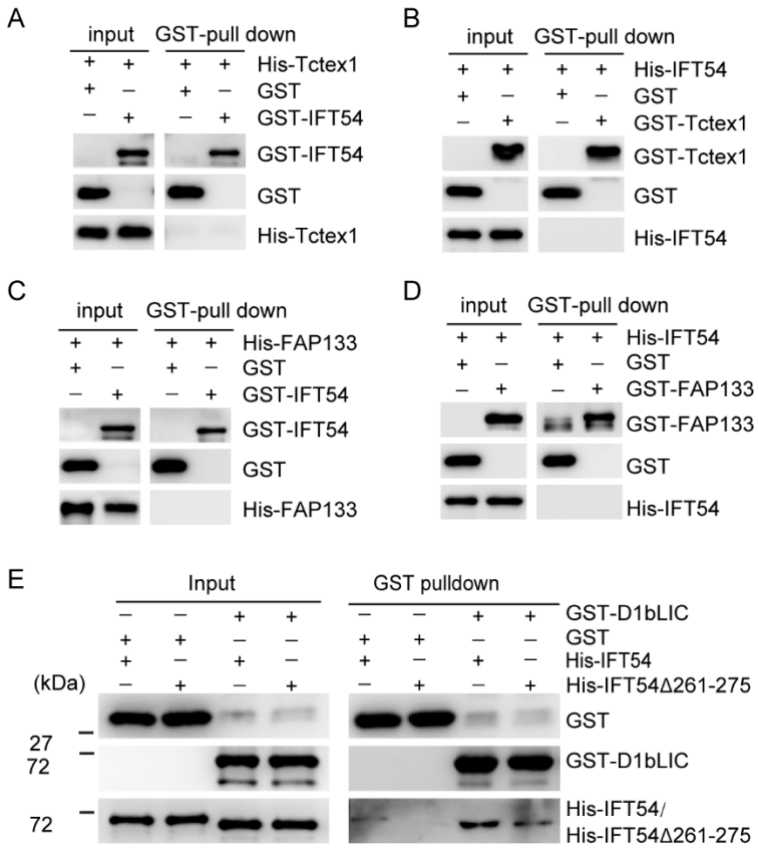

Appendix Figure S2. GST-pulldown assays for analyzing the interaction between IFT54 and IFT dynein subunits Tctex1, FAP133 or D1bLIC.

(A-B) Tctex1 does not interact with IFT54. (A) Bacterial expressed GST and GST-IFT54 were mixed with His-Tctex1 respectively followed by GST-pulldown and immunoblotting with anti-GST and anti-His antibodies, respectively. (B) Reciprocally, bacterial expressed GST and GST-Tctex1 were mixed respectively with His-IFT54 followed by GST-pulldown and immunoblotting with anti-GST and anti-His antibodies, respectively (B).

(C-D) FAP133 does not interact with IFT54. (C) Bacterial expressed GST and GST-IFT54 were mixed respectively with His-FAP133 followed by GST-pulldown and immunoblotting with anti-GST and anti-His antibodies, respectively. (D) Reciprocally, bacterial expressed GST and GST-FAP133 were mixed with respectively His-IFT54 followed by GST-pulldown and immunoblotting with anti-GST and anti-His antibodies, respectively.

(E) D1bLIC interacts with IFT54. Bacterial expressed GST and GST-D1bLIC were mixed His-IFT54 or His-IFT54$^{\Delta 261\text{-}275}$ respectively followed by GST pulldown and immunoblotting with anti-GST and anti-His antibodies, respectively.

Appendix Table S1. Primary antibodies used in this study

Antibody	Dilution		Reference or source
	IB	IF	
Rat anti-HA	1:1000	1:50	clone 3F10, Roche
Mouse anti-α-tubulin	1:3000	1:100	Cat# T6199, Sigma
Mouse anti-IC2	1:20000	NA	Cat# D6168, Sigma
Mouse anti-GST	1:2000	NA	Cat# BE2013, Abmart
Mouse anti-His	1:2000	NA	Cat# BE2019, Abmart
Mouse anti-GFP	1:2000	NA	Cat# N20004S, Abmart
Mouse anti-IFT139	1:10000	NA	(Cole et al., 1998)
Rabbit anti-IFT121	1:1000	NA	(Zhu et al., 2017a)
Rabbit anti-IFT43	NA	1:50	(Zhu et al., 2017a)
Rabbit anti-IFT172	1:2000	NA	This study
Rabbit anti-IFT38	1:2000	1:50	(Wu et al., 2018)
Rabbit anti-D1bLIC	1:1000	1:100	(Zhu et al., 2017b)
Rabbit anti-FLA8	1:2000	NA	(Liang et al., 2014)
Rabbit anti-FLA10	1:1000	1:100	(Meng and Pan, 2016)
Rabbit anti-KAP	1:1000	NA	(Liang et al., 2018)
Rabbit anti-KIF3A	1:2000	NA	Cat# B11259, Abcam
Rabbit anti-DYNC2LI1	1:2000	NA	Cat# 15949-1-AP, Proteintech

IF, immunofluorescence; NA, not applicable; IB, Immunoblot.

References

Cole, D.G., D.R. Diener, A.L. Himelblau, P.L. Beech, J.C. Fuster, and J.L. Rosenbaum. 1998. Chlamydomonas kinesin-II-dependent intraflagellar transport (IFT): IFT particles contain proteins required for ciliary assembly in Caenorhabditis elegans sensory neurons. *J. Cell Biol.* 141:993-1008.

Liang, Y., Y. Pang, Q. Wu, Z. Hu, X. Han, Y. Xu, H. Deng, and J. Pan. 2014. FLA8/KIF3B phosphorylation regulates kinesin-II interaction with IFT-B to control IFT entry and turnaround. *Dev. Cell*. 30:585-597.

Liang, Y., X. Zhu, Q. Wu, and J. Pan. 2018. Ciliary Length Sensing Regulates IFT Entry via Changes in FLA8/KIF3B Phosphorylation to Control Ciliary Assembly. *Curr. Biol.* 28:2429-2435 e2423.

Meng, D., and J. Pan. 2016. A NIMA-related kinase, CNK4, regulates ciliary stability and length. *Mol. Biol. Cell*. 27:838-847.

Wu, Q., K. Gao, S. Zheng, X. Zhu, Y. Liang, and J. Pan. 2018. Calmodulin regulates a TRP channel (ADF1) and phospholipase C (PLC) to mediate elevation of cytosolic calcium during acidic stress that induces deflagellation in Chlamydomonas. *FASEB J.* 32:3689-3699.

Zhu, B., X. Zhu, L. Wang, Y. Liang, Q. Feng, and J. Pan. 2017a. Functional exploration of the IFT-A complex in intraflagellar transport and ciliogenesis. *PLoS Genet.* 13:e1006627.

Zhu, X., Y. Liang, F. Gao, and J. Pan. 2017b. IFT54 regulates IFT20 stability but is not essential for tubulin transport during ciliogenesis. *Cell. Mol. Life Sci.* 74:3425-3437.